

# 000 Real-time pulse rate variability for remote autonomic assessment.

001  
002 Pedro Constantino  
003 pedroc\_24@hotmail.com  
004 João Sanches  
005 http://users.isr.ist.utl.pt/~jmrs/  
006

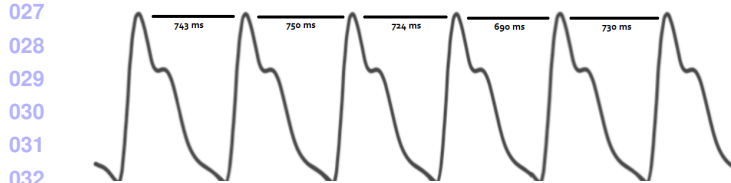
Institute for Systems and Robotics  
Instituto Superior Técnico  
Lisboa, Portugal

## 007 Abstract

008 Remote medicine is an emerging and important field with the potential  
009 to improve patients' health at the distance of a teleconsultation. Here, we  
010 propose a novel remote photoplethysmography algorithm suited to extract  
011 pulse rate variability in real-time from the face of a patient that is being  
012 recorded by a consumer-grade webcam. Because the autonomic nervous  
013 system plays a big role in regulating the human heart rate, a remote, real-  
014 time pulse rate variability sensor might be of interest for telepsychology  
015 and telepsychiatry alike. We test the real-time algorithm with an exper-  
016 iment where both PPG and rPPG are recorded at the same time, from a  
017 bluetooth PPG finger sensor and a computer webcam pointed at the face,  
018 respectively and where we can see that both signals have similar period-  
019 icity, a part from a phase difference.

## 021 1 Introduction

022 For several years physicians have monitored heart rhythms through aus-  
023 cultation and have noted that beat-to-beat times shift depending on age,  
024 illness and psychological state [1]. Both electrocardiography and photo-  
025 pletysmography are used to access cardiovascular signals (see Fig. 1).



027 Figure 1: Five time differences (in milliseconds) between six pulses via  
028 photoplethysmography. This figure is not in scale.

029 But, while the electrocardiogram is a measure of electrical activity di-  
030 rectly related to the contractions of muscular heart, the photoplethysmog-  
031 raphic signal is an optical measure that captures the amount of blood  
032 coming and going from a given tissue, and thus only indirectly it captures  
033 the heart's beating. From electrocardiography, heart rate (HR) is defined  
034 as the number of heartbeats per minute and heart rate variability (HRV)  
035 concerns the fluctuation in the time intervals between adjacent heartbeats  
036 [5]. Similarly, we can define pulse rate (PR) and pulse rate variability  
037 (PRV) in the context of photoplethysmography.

038 In 2018, remote photoplethysmography (rPPG) was reportedly [6] the  
039 most popular name for a technique that can also be referred to as contact-  
040 less PPG, camera-based PPG or imaging PPG. Aside from a source of  
041 light, the only component needed is a camera (e.g. low-cost webcam,  
042 mobile phone camera), which makes this technique really promising for  
043 the telemedicine context.

### 050 1.1 Heartbeat and autonomic regulation

051 Two types of cardiac muscle cells generate the heartbeat: (1) contractile  
052 cells produce strong contractions that cause the heart chamber to shrink  
053 and propel blood, and (2) specialized noncontractile muscle cells of the  
054 conducting system control modulate contractile cells. Contractile muscle  
055 cells, which comprise the majority of cardiac muscle cells, are activated  
056 by external action potentials, similarly to skeletal muscle. On the other  
057 side, noncontractile muscle cells are less in number and organized as a  
058 network made up of two types of cells: nodal cells and conducting cells.  
059 Nodal cells are autorhythmic, i.e. they contract on their own, without  
060 neural or hormonal stimulation, and generate the pacemaker potentials  
061 responsible for initiating the muscular heartbeat. They are located at the  
062 Sinoatrial (SA) and Atrioventricular (AV) nodes. However, nodal cells  
from the SA node naturally depolarize faster, 70–80 action potentials per

minute, than those in the AV node, 40–60 action potentials per minute,  
being the effective pacemaker cells in the heart. [4]

Although the SA node spontaneously generates the normal heartbeat  
cardiac rhythm, autonomic motor neurons, circulating hormones and ions  
can influence the inter-beat interval and magnitude of the myocardial con-  
traction [34]. More specifically, the cardiovascular center, located in the  
brain stem, integrates sensory information from various bodily receptors  
and responds through sympathetic and parasympathetic motor neurons  
(and endocrine systems), adjusting the HR continuously [3]. See Fig. 2.

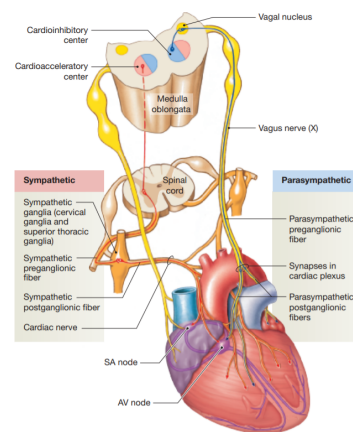


Figure 2: Autonomic innervation of the heart. Adapted from (Martini,  
2018).

Cardiac sympathetic nerves target the SA node, AV node, and the bulk  
of the myocardium and trigger norepinephrine and epinephrine release  
and binding to beta-adrenergic ( $\beta$ ) receptors located on cardiac muscle  
fibers, speeding up spontaneous depolarization in the SA and AV nodes  
(increasing HR) [2]. The parasympathetic vagus (X) nerves also innervate  
the SA node, AV node, and atrial cardiac muscle and trigger acetylcholine  
release and binding to muscarinic receptors, decreasing the rate of spon-  
taneous depolarization in the SA and AV nodes (slowing HR) [7].

## 2 Method

The proposed method takes as input a timestamped stream of video, i.e.  
a sequence of tuples of the form  $(frame[i], timestamp[i])$ , where  $i$  is the  
counter of video frames captured,  $frame[i]$  is a  $(width, height, 3)$  matrix  
storing each pixel's RGB intensities and  $timestamp[i]$  is the time at which  
the corresponding  $frame[i]$  was captured. It is assumed that all frames of  
the video contain a face.

First, for every video frame,  $frame[i]$ , an average of the RGB chan-  
nels over a predicted facial skin region of interest,  $avg\_rgb[i]$ , is produced.  
This can be accomplished with face detection, facial landmarks prediction  
and ROI selection, as seen in fig. 3.

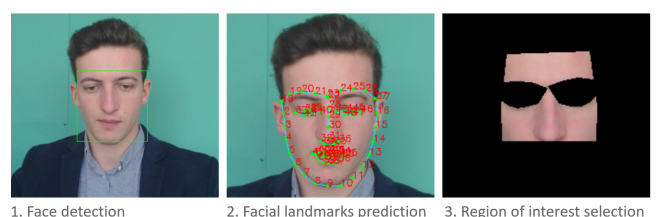


Figure 3: The first three steps of the algorithm.

Here, the regions comprising the cheeks, the nose and the forehead  
are considered, while the regions for beard and eyes are removed. Since

following algorithms assume that samples are evenly distributed in time, resampling the asynchronous RGB signal is needed.

After that, we must estimate a blood volume pulse (BVP) signal,  $bvp[t]$ , from the collected RGB signal,  $avg\_rgb[i]$ . For that we apply the POS method to transform the skin RGB signal into a BVP signal [9]. The POS method can be found in the chrominance category of rPPG algorithms, which means this algorithm integrates skin tone knowledge *a priori*, i.e. it requires less knowledge of the BVP signature and is more tolerant to distortion. A bandpass filter is further applied to clean the signal for peak detection. Cut off frequencies were set as [0.8, 2.5] Hz, since these frequencies correspond to a normal human heart rate range of 48 to 150 bpm. See fig. 4.

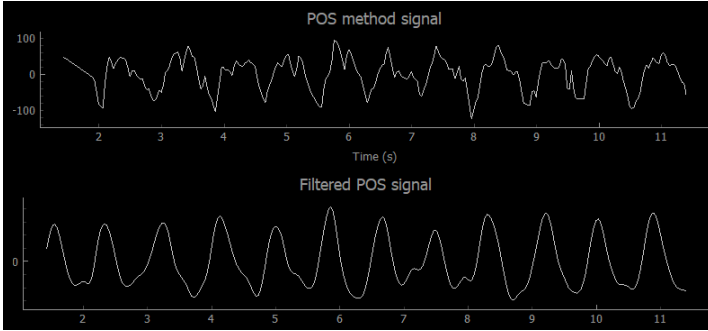


Figure 4: On the top, we can see the blood volume pulse obtained from the RGB signal via the POS method and, below, we see the filtered BVP.

Lastly, PR and its variability are estimated via the filtered BVP signal. Peak detection is firstly applied to the BVP signal in order to detect true heartbeats and, from the peaks, we can compute PP intervals. See fig. 5.

We extract PP intervals as the difference between pairs of consecutive peaks.

$$PPinterval_i = IBI_i = PeakTime_i - PeakTime_{i-1} \quad (1)$$

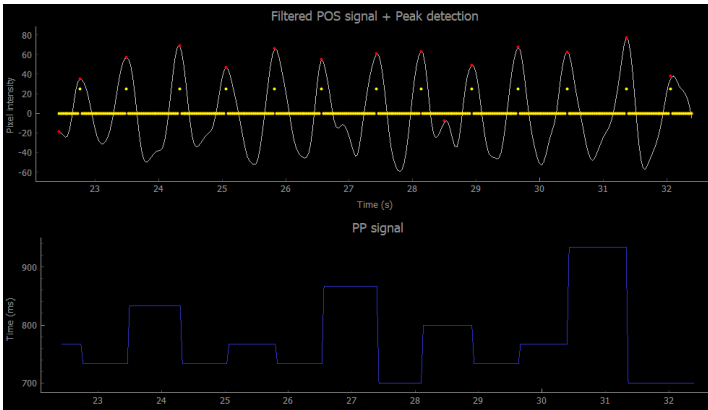


Figure 5: On the top, we can see the peak detection; below, we see the PP signal, or IBI signal.

From the PP intervals, we can provide estimations of PR and time-domain measures of PRV. For a full review on PRV metrics see [8].

### 3 Results and Discussion

To test the proposed algorithm, a standard grade laptop (MSI GF63 8RD) runs the whole rPPG pipeline in real-time using the embedded webcam as video input in one thread, and, on another thread, it acquires the traditional PPG signal from a pulse oximeter finger clip sensor, i.e. the ground truth signal. The PPG acquisition is mediated through a BITalino board, which stores the data at a constant rate and sends it via bluetooth to the laptop. In the end, we can display both signals at the same time and confirm that the rPPG signal follows the PPG signal closely (see Fig. 6), though we can see that the two signals are not perfectly aligned. This delay might be related with: 1) PPG thread starting acquisition first than the webcam thread, or vice versa and 2) the amount of time blood takes to travel from the heart to the face is different from the time it takes travelling from the

heart to the finger, and their also target of regulation by the circulatory system control mechanisms. Anyway, we can see that for every PPG-sensor pulse we can count a corresponding delayed rPPG-sensor pulse, confirming the ability of the proposed real-time algorithm to capture pulse rate variability, just like traditional PPG can do.

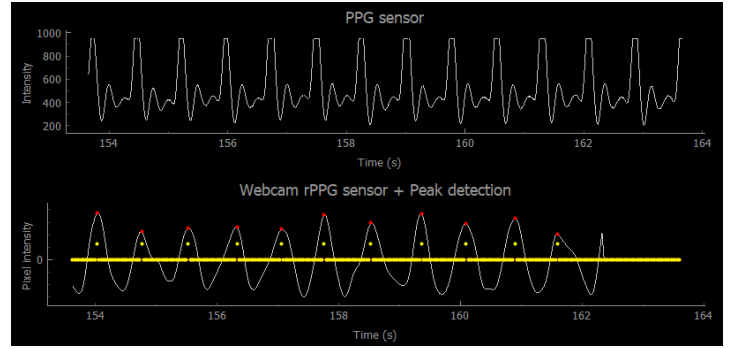


Figure 6: Real-time comparison of the photoplethysmography signal obtained through the finger clip sensor (upper panel) and the remote photoplethysmography signal obtained from the webcam video.

### 4 Conclusions

Virtually all published work on rPPG is based on offline computations. Accomplishing real-time pulse rate variability means that we can inspect the raw signal and PRV features during recording, which allows to identify artifacts, make sense of the values and overall have control over the precision of the process. Plus, a real-time rPPG algorithm ensures the doctor has some control over the quality of the measurement. The real-time display not only allows him to search for a sweet spot in terms of patient positioning and ambient lighting, but also to control overall quality of the record. This work is relevant because telemedicine is an emerging, cheaper form of providing health services and reliable tools must be developed to support doctors in making decisions within the remote context. In the future, it should be tested whether PRV features produced by the algorithm correlate with different groups of psychiatric patients.

### References

- [1] Gary G Berntson, J Thomas Bigger Jr, Dwain L Eckberg, Paul Grossman, Peter G Kaufmann, Marek Malik, Haikady N Nagaraja, Stephen W Porges, J Philip Saul, Peter H Stone, et al. Heart rate variability: origins, methods, and interpretive caveats. *Psychophysiology*, 34(6):623–648, 1997.
- [2] HF Brown, Dario DiFrancesco, and SJ Noble. How does adrenaline accelerate the heart? *Nature*, 280(5719):235–236, 1979.
- [3] BCB Fred Shaffer PhD and John Venner MAE. Heart rate variability anatomy and physiology. *Biofeedback (Online)*, 41(1):13, 2013.
- [4] Frederic H. Martini, Judi Lindsley Nath, Edwin F. Bartholomew, and William C. Ober. *Fundamentals of anatomy & physiology*. Pearson, 2018.
- [5] Rollin McCraty and Fred Shaffer. Heart rate variability: new perspectives on physiological mechanisms, assessment of self-regulatory capacity, and health risk. *Global advances in health and medicine*, 4(1):46–61, 2015.
- [6] Philipp V Rouast, Marc TP Adam, Raymond Chiong, David Cornforth, and Ewa Lux. Remote heart rate measurement using low-cost rgb face video: a technical literature review. *Frontiers of Computer Science*, 12(5):858–872, 2018.
- [7] Bert Sakmann, A Noma, and W Trautwein. Acetylcholine activation of single muscarinic k+ channels in isolated pacemaker cells of the mammalian heart. *Nature*, 303(5914):250–253, 1983.
- [8] Fred Shaffer and James P Ginsberg. An overview of heart rate variability metrics and norms. *Frontiers in public health*, 5:258, 2017.
- [9] Wenjin Wang, Albertus C den Brinker, Sander Stuijk, and Gerard De Haan. Algorithmic principles of remote ppg. *IEEE Transactions on Biomedical Engineering*, 64(7):1479–1491, 2016.

063  
064  
065  
066  
067  
068  
069  
070  
071  
072  
073  
074  
075  
076  
077  
078  
079  
080  
081  
082  
083  
084  
085  
086  
087  
088  
089  
090  
091  
092  
093  
094  
095  
096  
097  
098  
099  
100  
101  
102  
103  
104  
105  
106  
107  
108  
109  
110  
111  
112  
113  
114  
115  
116  
117  
118  
119  
120  
121  
122  
123  
124  
125  
\*/